Grenze International Journal of Engineering and Technology, Jan 2018

Study of 3D Mathematical Model of Rectangular Bar under Magnetostriction

Awani Bhushan[1], S.K. Panda[2], Yash Mittal[3], Peela Kartheek[4] and Rajat Kumar[5]
[1]Research scholar Department of Mechanical Engineering IIT (BHU) Varanasi, India
Email: abhushan.rs.mec13@itbhu.ac.in
[2]Associate Professor, Department of Mechanical Engineering, IIT (BHU) Varanasi, India
Email: skpanda.mec@itbhu.ac.in
[3-5]UG Student, Department of Mechanical Engineering, IIT (BHU) Varanasi, India
Emails: Yash.mittal.mec14@iitbhu.ac.in, Peela.kartheekcd.mec14@iitbhu.ac.in, Rajat.kumarcd.mec14@itbhu.ac.in

***Abstract*—This work addresses the Magnetostrictive effect in ferromagnetic components. Due to extensive use of ferromagnetic materials in practical engineering such as transducers, nuclear reactors, aerospace components and electric motor where magnetic field is dominant, this strain cannot be neglected. This work signifies the modelling and simulation of the three dimensional rectangular bar, fixed at one end and subjected to external magnetic field. The stress and strain developed due to magnetostrictive effect are simulated and dependency of the mathematical model has been observed on different parameters like magnetic field and current density with respect to strain. The magnetostrictve material surrounded by drive coil modelled as homogenized current carrying domain. The flux leakage is minimized by modelling a steel housing to create closed magnetic flux path. The problem is modeled and simulated in combined study of Magnetic Field and Static Structure in COMSOL Multiphysics 5.2. Result obtained involves significant strain in the core which can't be ignored in the engineering applications and can affect various design parameters if ignored. The strain caused due to magnetostrictive effect has been verified by existing empirical strain model.**

***Index Terms*— Magnetostriction, FEM, Magneto elasticity, Magnetization, Magnetic flux.**

I. INTRODUCTION

Magnetostriction is the phenomenon of change in dimension due to alignment of dipoles when subjected to external magnetic field. This phenomenon was discovered by J. Joule in 1842. This is observed in ferromagnetic and ferrimagnetic materials with significant magnitude of strain in the structure. Due to magnetic field the material change their shape and when they are stretched or compressed their magnetic energy changes [1]. Due to the widespread use of ferromagnetic materials in practical engineering, it has become increasingly important to explore their mechanical behavior under Magnetostriction. Ferromagnetic steel, for example, is a typical soft ferromagnetic widely used in nuclear reactors or some high magnetic field area, where the analysis of its magnetoelastic performance has always been a vital aspect of the structural design [2,3]. With technological advancement in the last few decades, many new types of functional ferromagnetic material emerge, such as the giant magnetostrictive alloy (with rare earth elements) [4,5],

Grenze ID: 01.GIJET.4.1.4

ferromagnetic shape memory alloys [6] magnetostrictive composites [7]. Such superior properties of magnetic materials have been employed to make sensors, actuators, and transducers. Correspondingly, the field of magnetostriction and magneto elasticity has been substantially grown [8-10]. The mechanical behavior of ferromagnetic plates and inductance winding structures has been studied by Moon et al. [11-15] in systematic manner. The experimental results revealed, for the first time, the magnetoelastic buckling of a ferromagnetic plate under a transverse magnetic field. Magnetostriction of ferromagnetic materials describes the change of their shape or dimension in response to the reorientation of magnetization under the influence of external magnetic field [16].

In this manuscript, mathematical modeling and simulation of the fixed end three dimensional rectangular bar subjected to external magnetic field is observed. The stress and strain distribution of magnetostrictive core has been presented and mathematical model is studied to observe the variation of parameters like magnetostriction with external magnetic field. The problem is modeled and simulated in combined study of Magnetic Field and Static Structure in COMSOL Multiphysics 5.2.

II. MATHEMATICAL BACKGROUND

Consider a magnetostrictive rectangular bar of length L and area of cross section A. Upon application of external magnetic field H, change in length of the bar be ΔL as shown in the Fig. 1.

The conditions required for the given phenomenon involves

- This phenomenon is more visible in the case of the giant magnetostrictive material.
- Magnetic field should be in the direction of mechanical extension.
- Mechanical boundary conditions must be specified in order to observe the stress or strain as a result of extension.

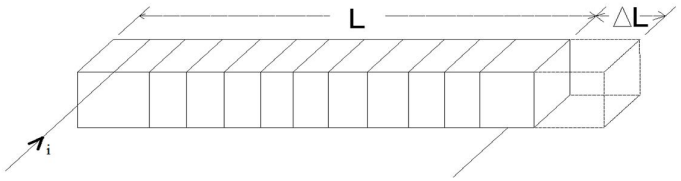

Fig. 1 : Magnetostriction in the bar

The purpose of mathematical modelling involves to predict the behavior of the magnetostrictive material in Magneto-elastic condition. The strain is developed due to both the external magnetic field and applied mechanical stresses.

The constitutive magnetostriction equation are:

$$S = \eta_H.T + d.H \tag{1}$$

$$B = d.T + \mu_T.H \tag{2}$$

The following parameters are considered to be constant: $\eta_H = \eta$ and $\mu_T = \mu$

We consider the strain is only in X-direction,

Let the position of the point is given by, $u = f(x, y, z)$

Strain is given by, $S = \frac{\partial u}{\partial x}$ (3)

Derivating the equation (1) twice with respect to time‘t’

$$\frac{\partial^2 S}{\partial t^2} = \eta \frac{\partial^2 T}{\partial t^2} + d \frac{\partial^2 H}{\partial t^2} \tag{4}$$

Substituting the equation (3) in equation (4)

$$\frac{\partial}{\partial x}\left(\frac{\partial^2 u}{\partial t^2}\right) = \eta \frac{\partial^2 T}{\partial t^2} + d \frac{\partial^2 H}{\partial t^2} \tag{5}$$

Considering Newton’s second law $F = (m \cdot a)$ and we know stress $T = F / A$

$$\frac{\partial T}{\partial x} = \frac{\partial (F / A)}{\partial x} = \frac{\partial F}{\partial V} = \frac{\partial (m \cdot a)}{\partial V} = \rho \cdot a = \rho \cdot \frac{\partial^2 u}{\partial t^2} \tag{6}$$

Differentiating equation (6) w.r.t x

$$\frac{\partial^2 T}{\partial x^2} = \frac{\partial}{\partial x}\left(\rho \frac{\partial^2 u}{\partial t^2}\right) = \rho \frac{\partial}{\partial x}\left(\frac{\partial^2 u}{\partial t^2}\right) = \rho\eta \frac{\partial^2 T}{\partial t^2} + \rho d \frac{\partial^2 H}{\partial t^2} \tag{7}$$

$$\frac{\partial^2 T}{\partial x^2} = \rho\eta \frac{\partial^2 T}{\partial t^2} + \rho d \frac{\partial^2 H}{\partial t^2} \tag{8}$$

Maxwell's equations are

$$\nabla \times E = -\frac{\partial B}{\partial t} \tag{9}$$

$$\nabla \times B = \mu J + \mu\varepsilon \frac{\partial E}{\partial t} \tag{10}$$

Taking '∇' operator on both sides of equation (9)

$$\nabla \times (\nabla \times B) = \mu (\nabla \times J) + \mu\varepsilon \frac{\partial (\nabla \times E)}{\partial t} \tag{11}$$

From Ohm's law we know that $J = \sigma E$

$$\nabla (\nabla \cdot B) - \nabla^2 B = \mu (\nabla \times J) + \mu\varepsilon \frac{\partial (\nabla \times E)}{\partial t} \tag{12}$$

We know that $(\nabla . B) = 0$

$$-\nabla^2 B = \mu (\nabla \times J) + \mu\varepsilon \frac{\partial (\nabla \times E)}{\partial t} \tag{13}$$

$$-\nabla^2 B = \mu (\nabla \times \sigma E) + \mu\varepsilon \frac{\partial (\nabla \times E)}{\partial t} \tag{14}$$

$$-\nabla^2 B = \mu\sigma (\nabla \times E) + \mu\varepsilon \frac{\partial (\nabla \times E)}{\partial t} \tag{15}$$

$$-\nabla^2 B = \mu\sigma\left(-\frac{\partial B}{\partial t}\right) + \mu\varepsilon \frac{\partial}{\partial t}\left(-\frac{\partial B}{\partial t}\right) \tag{16}$$

$$\frac{1}{\mu}(\nabla^2 B) = \sigma\left(\frac{\partial B}{\partial t}\right) + \varepsilon \frac{\partial}{\partial t}\left(\frac{\partial B}{\partial t}\right)$$

$$\frac{1}{\mu}(\nabla^2 (dT + \mu H)) = \sigma \frac{\partial}{\partial t}(dT + \mu H) + \varepsilon \frac{\partial^2}{\partial t^2}(dT + \mu H) \tag{17}$$

$$\frac{d}{\mu}\nabla^2 T + \nabla^2 H = \sigma \frac{\partial}{\partial t}(dT + \mu H) + \varepsilon \frac{\partial^2}{\partial t^2}(dT + \mu H) \tag{18}$$

$$\frac{d}{\mu}\left(\frac{\partial^2 T}{\partial x^2}\right) + \nabla^2 H = \sigma \frac{\partial}{\partial t}(dT + \mu H) + \varepsilon \frac{\partial^2}{\partial t^2}(dT + \mu H) \tag{19}$$

$$\frac{d}{\mu}\left(\rho\eta \frac{\partial^2 T}{\partial t^2} + \rho d \frac{\partial^2 H}{\partial t^2}\right) + \nabla^2 H = \sigma \frac{\partial}{\partial t}(dT + \mu H) + \varepsilon \frac{\partial^2}{\partial t^2}(dT + \mu H) \tag{20}$$

$$\nabla^2 H = \sigma \frac{\partial}{\partial t}(dT + \mu H) + \varepsilon \frac{\partial^2}{\partial t^2}(dT + \mu H) - \frac{d\rho\eta}{\mu}\frac{\partial^2 T}{\partial t^2} - \frac{\rho d^2}{\mu}\frac{\partial^2 H}{\partial t^2} \tag{21}$$

$$\nabla^2 H = \sigma d \frac{\partial T}{\partial t} + \sigma\mu \frac{\partial H}{\partial t} + \varepsilon d \frac{\partial^2 T}{\partial t^2} + \varepsilon\mu \frac{\partial^2 H}{\partial t^2} - \frac{d\rho\eta}{\mu}\frac{\partial^2 T}{\partial t^2} - \frac{\rho d^2}{\mu}\frac{\partial^2 H}{\partial t^2} \tag{22}$$

$$\nabla^2 H = \sigma d \frac{\partial T}{\partial t} + \frac{d}{\mu}(\mu\varepsilon - \rho\eta)\frac{\partial^2 T}{\partial t^2} + \sigma\mu \frac{\partial H}{\partial t} + \left(\frac{\mu^2\varepsilon - \rho d^2}{\mu}\right)\frac{\partial^2 H}{\partial t^2} \tag{23}$$

When the system is exposed to harmonic excitation then the equations (23) and (8) simplifies to the following

$$\frac{\partial^2 T}{\partial x^2} = \omega^2 G_1 T + \omega^2 G_2 H \quad (24)$$

$$\nabla^2 H = \omega^2 k_1 T + \omega^2 k_2 H \quad (25)$$

Where, $G_1 = -\rho\sigma$, $G_2 = -\rho d$ and

$$k_1 = \frac{\left(d\left(\rho\eta - \mu\varepsilon\right) + \frac{i\mu\sigma d}{\omega}\right)}{\mu}, \quad k_2 = \frac{\left(\left(\rho d^2 - \mu^2\varepsilon\right) + \frac{i\mu^2\sigma}{\omega}\right)}{\mu}$$

Now we can consider the parameters used above with some iterative evaluation with H and T. η changes with the value of H, with new value of H the value of T is changed, With new T the value of μ is changed, With new μ the value of H is changed and this iteration is done till constant values of $\eta_{(H)}$ and $\mu_{(T)}$ are obtained.

III. Finite Element Model

The model contains the steel housing enclosing a drive coil. In the core there is rectangular magnetostrictive material which undergo the influence of magnetic field produced by passing a current through the drive coil. An air domain is developed around the steel housing to realistically model the magnetic flux path. The steel housing helps in minimizing flux leakage by creating a closed magnetic flux path. The current in the coil was considered to be DC, so the analysis was performed in stationary state. One end of the core material was fixed to study mechanical stresses. To specify magnetic constitutive relation in steel housing, the nonlinear HB curve was obtained by choosing Soft Iron material without losses. Similarly nonlinear HB relation was also used for magnetostrictive material by importing the text file which is used to create an interpolation function that can provide the corresponding values of Magnetic field (H) for the given magnetic flux density (B).

Table I. Properties of Magnetostrictive Material

Description	Value	Material Property
Young's modulus	60 x 10^9 Pa	E
Electric conductivity	0	σ
Density	7870 kg/m3	ρ
Magnetostriction constant	2 x 10^{-4}	λ_s
Poisson's ratio	0.3	ν
Saturation magnetization	15 x 10^5 A/m	M_{sat}
Relative permittivity	1	ε_r

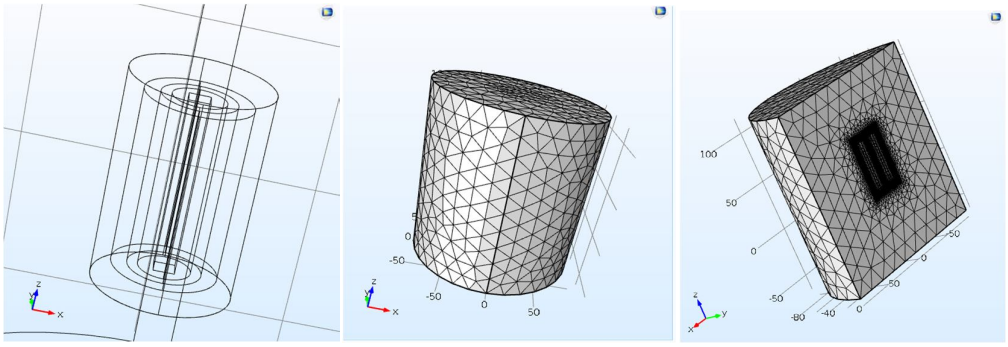

(a) (b) (c)

Fig. 2 (a) Wireframe model of 3D Bar with Steel housing and Meshed model (b) Full Model (c) Half model

IV. Results and Discussion

The particular problem has been solved to observe the stress and strain distribution plot and various parametric studies has been taken place to characterize and validate the problem. The following Fig. 3(a) shows the z component of stress in the magnetostrictive core. This shows the development of stress in the end for a particular problem with the value 2 x 10^5 Pa, which is significant for the boundary condition. The distribution of Von-Mises stress has been plotted against the 3D core shown in Fig. 3(b) and in measurement developed in core with the value of 3.5 x 10^4Pa for a same problem. Fig. 3 (c) shows the z-component of strain in the magnetostrictive material. The maximum strain is observed at the free ends and different parametric studies lead to appropriate and significant strain in the body. Fig. 3(d) shows the plot of magnetic flux density in the region inside the housing including the magnetostrictive core. The following Fig. 4 (a) shows the variation of magnetostriction with applied external magnetic field. The magnetostriction reaches the saturation state of around 2.7x10^{-4} and the sharp nonlinear behavior has been observed in the region of the magnetic field in Z-direction. It also shows the characteristic λH curve of the magnetostrictive material obtained from the parametric study that simulated a quasi-statically increasing the current density in the coil. The reason is that the magnetic field is oriented along the Z direction, then only the Z-components of the magnetostriction and magnetic field are plotted here.

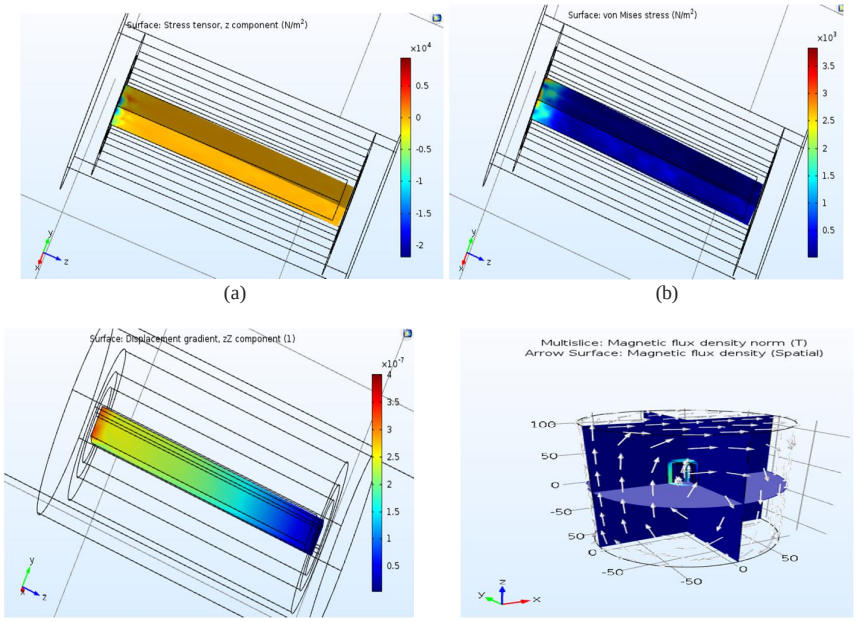

(a) (b)

(c) (d)

Fig. 3(a) Stress distribution in Z direction (b) Von-mises stress distribution, (c) Strain distribution in z-direction, (d) Magnetic flux density

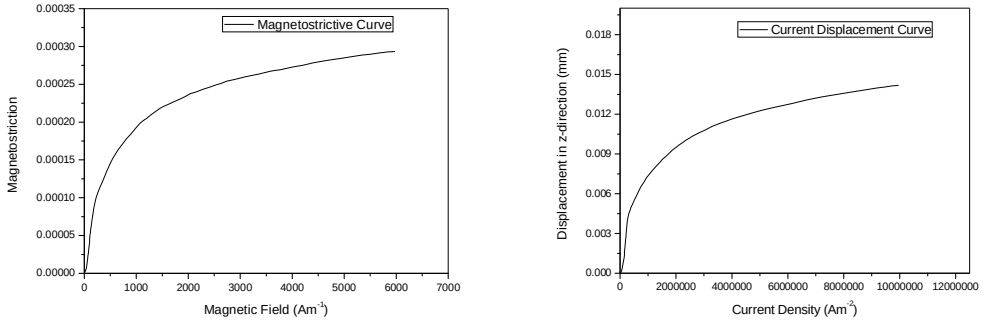

(a) (b)

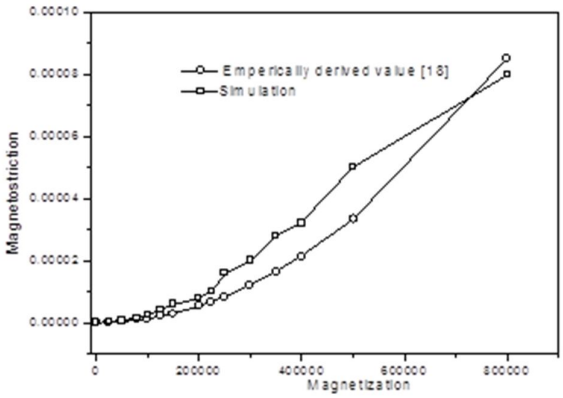

(c)

Fig. 4 (a) Magnetostriction is plotted against the Magnetic Field (Am-1) for bar and (b) Magnetostrictive deformation is plotted against the current density (J) for bar (c) Comparison of magnetostriction value obtained from simulation to empirically developed value

From the Fig. 4(a) we observe that the value of magnetostriction reaches a saturation value as we observe in the physical world. So irrespective of geometry the material should reach saturated magnetostriction value at some point and we can see this being validated with existing 2D magnetostrictive model [17]. Fig. 4 (b) shows the displacement in z-direction against the current density applied externally to the drive coil. This is very useful to determine the performance of a transducer. Fig. 4 (c) represents the comparison of the magnetostriction value estimated form simulation to the empirically derived magnetostriction results obtained from the following expression [18].

$$\lambda(t,x) = \frac{3}{2}\frac{\lambda_s}{M_s^2} M^2(t,x) \tag{26}$$

where, $\lambda(t,x)$ is magnetostriction value for the corresponding magnetization $M(t,x)$.

V. Conclusion

The 3D mathematical model has been developed and the distribution of various stresses and strain has been plotted due to magnetostriction for a particular problem. The significant strain is observed in the results of the magnetostrictive material. The magnetostriction should reach a saturation value which is an observed physical phenomenon through experiments and through simulations also we get the same. Further increase in external magnetic field doesn't increase the magnetostriction value of the core observed in parametric studies. The nature of the curves follows the existing standard results observed. The significant magnetostrictive strain in the core is observed which plays vital role in calibration of various engineering application and can affect various design parameters if ignored. The magnetostriction results has been validated with empirically derived results [18].

References

[1] Bailoni, M., "Mathematical Modelling and simulation of Magnetostrictive materials by COMSOL Multiphysics", COMSOL Conference, Hannover, 2008.
[2] Carroll, M. M., "The Foundation of Solid Mechanics", Appl. Mech. Rev. , Vol. 38, No. 10, 1986, pp. 1301–1308.
[3] Engdahl, G., "Handbook of giant magnetostrictive material", ISBN 0-12-238640-x, Academic Press, San Diego, 2000.
[4] Jiang, Z., "Development of the Giant Magnetostrictive Compound of Rare Earth and Iron", Chinese Journal of Rare Earth, Vol. 12, 1992, pp. 19-26, in Chinese.
[5] Jiles,D.C., The development of highly magnetostrictive rare earth-iron alloys, Journal of Physics D: Applied Physics, Vol. 27, No. 1,1994, pp. 1-11
[6] Moon, F. C., "Magneto Solid Mechanics", Wiley, New York, 1984.
[7] Nan, C. W., and Weng, G. J., "Influence of Microstructural Features on the Effective Magnetostriction of Composite Materials", Phys. Rev. B, 60, 1999, pp. 6723-6730.

[8] O'Handley, R. C., "Model for Strain and Magnetization in Magnetic Shape-Memory Alloys", J. Appl. Phys., 83, 1998, pp. 3263–3270.
[9] Fang, D., Wan, Y., Feng, X., Soh, A.K., Deformation and Fracture of Functional Ferromagnetics. Applied Mechanics Reviews 61, 2008, pp. 20803(1-23).
[10] Pao, Y. H., "Electromagnetic Force in Deformable Continua", Mechanics Today, N. Nasser, ed. Pergamon, Bath, 1978.
[11] Moon, F. C., and Pao, Y. H., "Magnetoelastic Buckling of a Thin Plate," ASME J. Appl. Mech., 35, 1968, pp. 53–58.
[12] Moon, F. C., "The Mechanics of Ferroelastic Plates in a Uniform Magnetic Field," ASME J. Appl. Mech., 37, 1970, pp. 153–158.
[13] Moon, F. C., "Buckling of a Superconducting Ring in a Toroidal Magnetic Field," ASME J. Appl. Mech., 46, 1979, pp. 151–155.
[14] Moon, F. C., and Swanson, C., "Experiments on Buckling and Vibration of Superconducting Coils," ASME J. Appl. Mech., 44, 1977, pp. 707–713.
[15] Pao, Y. H., and Yeh, C. S., "A Linear Theory for Soft Ferromagnetic Elastic Solids," Int. J. Eng. Sci., 11, 1973, pp. 415–436.
[16] Wang, H., Zhang, Y.N., Wu, R.Q., Sun, L.Z., Xu, D.S., Zhang, Z.D., "Understanding strong magnetostriction in Fe 100-xGaxalloys". Scientific Reports, 3, 2013, 1–5.
[17] "Nonlinear Magnetostrictive Transducer", COMSOL reference manual in Multiphysics 5.2, 2017, pp. 1-24.
[18] Dapino, M.J. , Smith, R.C. , Flatau, A.B., "Structural Magnetic Strain Model for Magnetostrictive Transducers", IEEE Transactions on Magnetics. 36, 2000, pp. 545–556.